http://dx.doi.org/10.21577/0103-5053.20180210

J. Braz. Chem. Soc., Vol. 30, No. 4, 793-803, 2019
Printed in Brazil - ©2019 Sociedade Brasileira de Química

Article

Zika Virus Activity of the Leaf and Branch Extracts of *Tontelea micrantha* and Its Hexane Extracts Phytochemical Study

***Fernanda L. Ferreira,[a] Marcela S. Hauck,[b] Lucienir P. Duarte,[a]*
José C. de Magalhães,[b] Louise S. M. da Silva,[a] Lúcia P. S. Pimenta,[a] Julio C. D. Lopes,[a]
Maria O. Mercadante-Simões[c] and Sidney A. Vieira Filho[d]***

[a]*Departamento de Química, Instituto de Ciências Exatas, Universidade Federal de Minas Gerais, 31270-901 Belo Horizonte-MG, Brazil*

[b]*Departamento de Química, Biotecnologia e Engenharia de Bioprocessos, Universidade Federal de São João del-Rei, Campus Alto Paraopeba, 36420-000 Ouro Branco-MG, Brazil*

[c]*Departamento de Biologia Geral, Centro de Ciências Biológicas e da Saúde, Universidade Estadual de Montes Claros, 39401-089 Montes Claros-MG, Brazil*

[d]*Departamento de Farmácia, Escola de Farmácia, Universidade Federal de Ouro Preto, Campus Morro do Cruzeiro, 35400-000 Ouro Preto-MG, Brazil*

The new triterpene friedelan-1,3,21-trione, the known compounds friedelan-3-one, 3β-friedelinol, 3,4-*seco*-friedelan-3-oic acid, 28-hydroxyfriedelan-3-one, friedelan-3-oxo-28-al, friedelan-3,21-dione, 30-hydroxyfriedelan-3-one, a mixture of 30-hydroxyfriedelan-3-one/21α-hydroxyfriedelan-3-one, 21β-hydroxyfriedelan-3-one, gutta-percha, squalene, and a mixture of palmitic/stearic/oleic acids were isolated from the hexane extracts of leaves and branches of *T. micrantha*. Their chemical structures were established by Fourier transform infrared spectroscopy (FTIR), gas chromatography (GC), 1D/2D nuclear magnetic resonance (NMR) and comparison with the literature data. All compounds were described for *T. micrantha* and the genus *Tontelea* for the first time. The branch and leaf extracts displayed anti-Zika virus activity at the lowest tested concentration of 15.6 μg mL^{-1}, mainly virucidal effect, and presented no cytotoxicity to Vero cells. Furthermore, the ethyl acetate and methanolic leaf extracts demonstrated the best activities at the concentration of 31.2 and 15.6 μg mL^{-1} at the viral adsorption and penetration stages, respectively. These results showed that these extracts may be promising candidates for the Zika virus treatment.

Keywords: *Tontelea micrantha*, Celastraceae, friedelan-1,3,21-trione, antiviral activity, Zika virus

Introduction

The Celastraceae family comprises about 106 genera with 1300 species.[1,2] Many Brazilian species of this family have been studied due to their use in traditional medicine and pharmacological properties.[2] *Tontelea micrantha* (Mart.) A.C.Sm. is a species of the Celastraceae family popularly known as "rufão" and is found in the Brazilian Cerrado, mainly in the north of Minas Gerais State. The alcoholic extracts of its roots are used in the traditional medicine for the treatment of kidney disturbs, and the fruit oils are employed to treat inflammatory processes.[3-5] Furthermore, its fruits are edible, suggesting low or even absent toxicity. Even though the literature[3] also describes the histochemical and pharmacognostic profile of the aerial and underground parts of *T. micrantha*, there are no reports of detailed chemical studies of this species or some other member of the *Tontelea* genus.

Phytochemical studies of the Celastraceae family led to the isolation of many bioactive secondary metabolites such as flavonoids, steroids and different classes of pentacyclic triterpenes. Also, many reports describe pharmacological properties of triterpenes like anti-inflammatory,[6,7] antiulcerogenic,[8] analgesic,[9] antibacterial, antifungal,

*e-mail: lucienir@ufmg.br

antiviral, antiparasitic, antioxidant, hepatoprotective, neuroprotective, insecticidal and others.[10] Moreover, some species are already employed in the treatments of gastric ulcers, presenting anti-inflammatory and analgesic activities such as *Maytenus ilicifolia* Mart. ex Reiss. and *M. aquifolium* Reiss.[11] Additionally, the hydroalcoholic leaf extract from *M. ilicifolia* was active against bovine herpesvirus type 5 and avian metapneumovirus.[12]

Viral infections represent an important target to the pharmacological research, especially aiming virus such as the Zika virus (ZIKV). Infections by ZIKV can be very serious and dangerous for pregnant women because it may induce microcephaly, a brain anomaly that causes a malformation of the brain and head of newborns, loss of pregnancy, stillbirth and other congenital disabilities.[13,14] In the years 2015-2016, an outbreak in Brazil occurred causing a 10-fold increase in newborns with microcephaly in comparison with previous years.[13-15] Unfortunately, there is no treatment or specific drugs against ZIKV until this moment. For these reasons, researches leading to potential antiviral substances are essential.[16,17] In this context, the Celastraceae family represents a source of high diversity for bioprospecting new substances with antiviral properties.

In the present work, the effect of leaf and branch extracts of *T. micrantha* against ZIKV was evaluated. Furthermore, the phytochemical study of the hexane extract of leaves and branches led to the identification of fourteen known compounds and the novel triterpene friedelan-1,3,21-trione (Figure 1), herein described for the first time. All compounds were characterized using spectroscopic analysis and comparison with the literature data.

Experimental

General procedures

Silica gel G-60 (0.25 mm, Merck) plates were used for thin layer chromatography (TLC), and silica gel 60 (0.063-0.200 mm, Merck) or silica flash (0.040-0.063 mm, Sigma-Aldrich) were employed for

Compound	R_1	R_2	R_3	R_4	R_5
1	=O	=O	CH_3	=O	CH_3
2	H	=O	CH_3	H	CH_3
3	H	OH	CH_3	H	CH_3
5	H	=O	CH_2OH	H	CH_3
6	H	=O	CHO	H	CH_3
7	H	=O	CH_3	=O	CH_3
8	H	=O	CH_3	H	CH_2OH
9	H	=O	CH_3	αOH	CH_3
10	H	=O	CH_3	βOH	CH_3

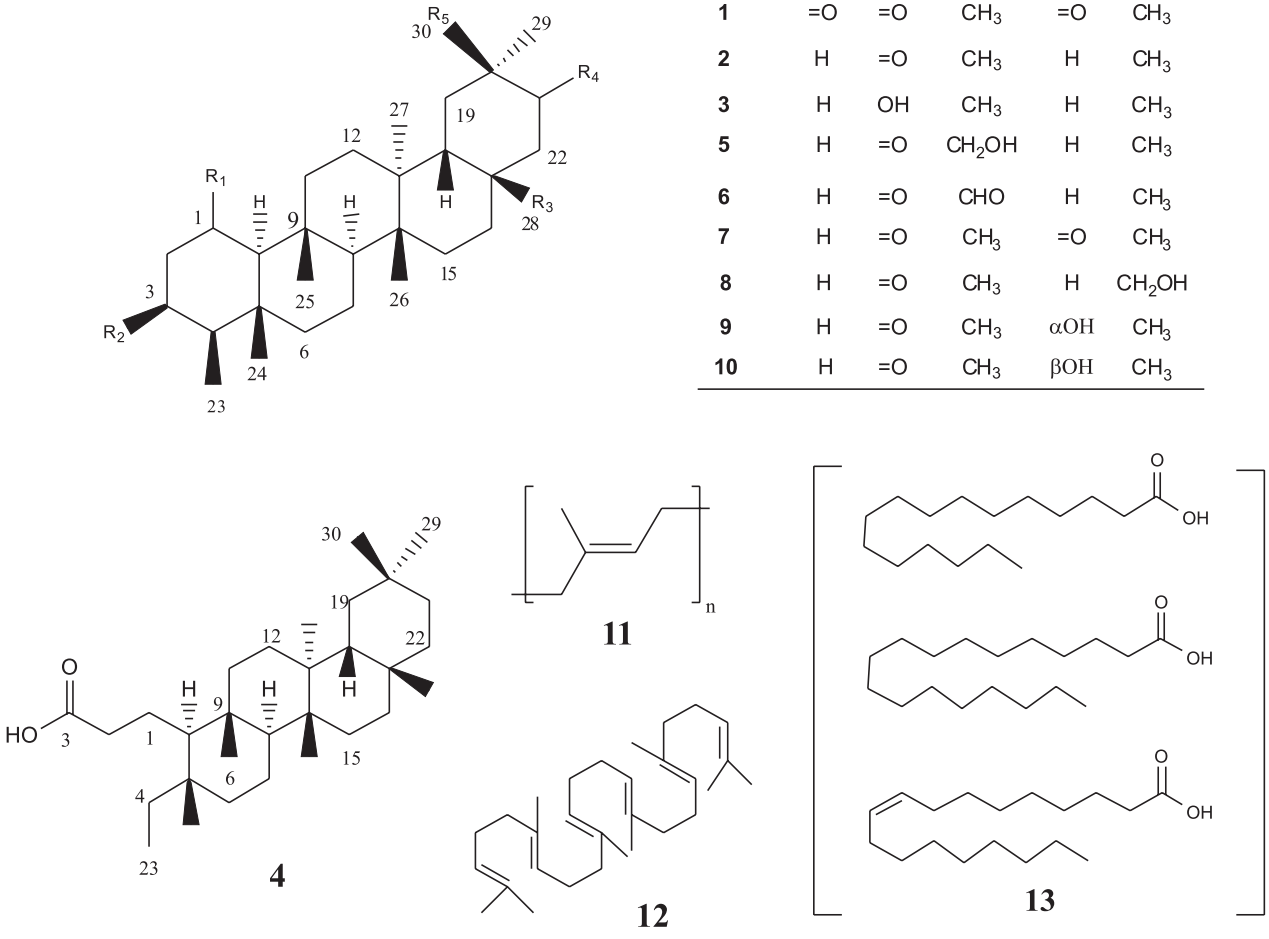

Figure 1. Chemical structures of compounds from hexane leaf and branch extracts of *Tontelea micrantha*.

column chromatography (CC). Hexane (Hex, Vetec), chloroform ($CHCl_3$, Vetec), ethyl acetate (EtOAc, Vetec) and methanol (MeOH, Vetec), pure or in gradient mixtures, were used as eluents. The ^1H (400 MHz) and ^{13}C (100 MHz) nuclear magnetic resonance (NMR) spectra were performed on a Bruker Avance DRX-400, operating at 300 K. The chemical shift assignments (δ) and the coupling constants (J) were expressed in ppm and Hz, respectively, using tetramethylsilane (TMS) as reference ($\delta_H = \delta_C = 0$). The samples were dissolved in $CDCl_3$ pure or with drops of Py-D_5. The infrared (IR) spectra (KBr, cm^{-1}) were obtained on a Shimadzu IR408 spectrometer. The melting points were determined using an MQAPF-302 (Microquímica Equipamentos Ltda.) apparatus. The optical rotation was measured on an ADP220 Bellinghan + Stanley Ltd. polarimeter. Liquid chromatography mass spectrometry (LC-MS) analysis was performed on a Bruker Daltonics (MicroTOF QII model) equipped with a high resolution electrospray ionization source and a time of flight analyzer (HR-ESI-TOF), operating in the positive ion mode. The gas chromatography (GC) analyses were performed on HP7820A (Agilent) system equipped with flame ionization detector (FID) and Supelcowax-10 column (15 m × 0.2 mm × 0.2 μm) (Supelco). The following analytical conditions were used: 1.0 μL of injected sample solution, column temperature at 120 °C (1 min) up to 240 °C (10 °C min^{-1}), injector at 250 °C, split 1:50, detector at 260 °C and H_2 (3.0 mL min^{-1}) as the carrier gas. Data acquisition was carried out using EZChrom Elite Compact Software 3.3.2 (Agilent). The sample (5.0 mg) was heated with 100 μL of 14% BF_3-methanol solution in a water bath (60 °C for 10 min), and the fatty acid methyl esters (FAME) were further extracted with hexane. This hexane solution was analyzed by GC-FID, and the observed retention times were compared with reference standards FAME (Supelco: 47885-U).

Plant material

Leaves and branches of *T. micrantha* were collected in Montes Claros, Minas Gerais State, Brazil. The plant was identified by the botanist Dr Maria Olívia Mercadante-Simões and a voucher specimen (No. BHCB 144.623) was deposited in the Herbarium of Departamento de Botânica, Instituto de Ciências Biológicas, Universidade Federal de Minas Gerais, Brazil.

Extraction and isolation

After dried at room temperature, samples of leaves and branches of *T. micrantha* were fragmented in a knife mill resulting in powders (720.0 g for leaves; 2.6 kg for branches) that were macerated with organic solvents further removed using a rotatory evaporator. The following extracts were obtained for the leaves: hexane (43.5 g), ethyl acetate (ELE, 45.0 g), and methanolic (MLE, 38.3 g). The following extracts were obtained for the branches: hexane (25.7 g), chloroform (CBE, 61.1 g) and ethyl acetate (EBE, 9.75 g). During the hexane removal, white solids precipitated from both extracts and were separated by filtration (WLS, 0.87 g from leaves, and WBS, 5.3 g from branches). These solids were further chromatographed.

TLC analysis of the hexane extracts from leaves and branches showed that both have an expressive amount of the polymer *trans*-1,4-polyisoprene (gutta-percha), which is very common in the Celastraceae family.[18] Rodrigues *et al*.[19] described an efficient method for gutta-percha removal from the extract, which consists in a silica gel CC exhaustively eluted with methanol followed by chloroform. The first elution using MeOH removes all compounds except gutta-percha that remains retained at the top of the column. Then, this polymer is isolated by eluting the column with chloroform.

Employing the methodology described by Rodrigues *et al*.,[19] the hexane extracts from the leaves (43.5 g) and branches (25.7 g) were chromatographed on silica gel CC, firstly with MeOH until the TLC analysis showed no more eluted compounds, and then with $CHCl_3$. The chloroform fractions from leaves and branches furnished gutta-percha (**11**) (20.3 and 1.5 g, respectively). The methanolic fraction from the leaves, after solvent removal with a rotatory evaporator, yielded 15.0 g of a greenish solid (HLE). Differently, the initial methanolic fraction from the branches presented a yellow color and it was reduced with a rotatory evaporator furnishing 2.2 g of a yellowish solid (YBS). Continuing the elution with MeOH, a further fraction was then separated until the TLC analysis showed no more eluted compounds, leading to a slightly greenish solid (HBE, 20.4 g) after solvent removal. All solids were further chromatographed.

The solid from the hexane leaf extract (WLS, 0.87 g) was subjected to silica gel CC (A) furnishing 101 fractions of 20 mL. The fractions A32-37 (Hex:$CHCl_3$ 65:35) yielded friedelan-3-one (**2**) (62.7 mg) and the fractions A39-48 (Hex:$CHCl_3$ 7:3) provided a mixture of compounds **2** and 3β-friedelinol (**3**) (324.0 mg).

The solid from the hexane branch extract (WBS, 5.3 g) was fractionated on silica gel CC (B) leading to 321 fractions of 15 mL. An additional amount of **2** (28.0 mg) was isolated from the fractions B136-153 ($CHCl_3$). Friedelan-3-oxo-28-al (**6**) (62.6 mg) was obtained from the fractions B167-180 ($CHCl_3$:EtOAc 85:15).

The fractions B181-189 ($CHCl_3$:EtOAc 8:2) yielded friedelan-3,21-dione (**7**) (2.2 g). The fractions B190-197 ($CHCl_3$:EtOAc 75:25, 0.96 g) were re-chromatographed on silica gel CC (C) and 111 fractions of the 10 mL were obtained. The fractions C33-34 ($CHCl_3$:EtOAc 9:1) furnished additional amount of **7** (18.0 mg). The fractions C35-43 ($CHCl_3$:EtOAc 85:15, 0.77 g) were submitted to a new CC (D, 78 fractions of the 15 mL) yielding **7** (5.2 mg) from the fraction D43 ($CHCl_3$:EtOAc 98:2) and friedelan-1,3,21-trione (**1**) (535.0 mg) from the fractions D45-50 ($CHCl_3$:EtOAc 85:15). The fractions B198-245 ($CHCl_3$:EtOAc 80:20, 1.17 g) were re-chromatographed on silica gel CC (E, 81 fractions of the 15 mL) providing a mixture (467.6 mg) of 30-hydroxyfriedelan-3-one (**8**) and 21α-hydroxyfriedelan-3-one (**9**) from the fractions E40-44 ($CHCl_3$:EtOAc 85:15). This mixture was purified on flash silica CC (F, 107 fractions of the 10 mL) yielding **8** (165.0 mg) from the fractions F64-67 ($CHCl_3$:EtOAc 90:10).

Part of the greenish solid from hexane leaf extract free of gutta (HLE) (14.0 g) was chromatographed on silica gel CC (G) furnishing 102 fractions of 200 mL. The fractions G1-6 (Hex) yielded squalene (**12**) (410.0 mg). The fractions G30-38 (Hex:$CHCl_3$ 8:2, 3.6 g) were subjected to a new silica gel CC (H) providing 88 fractions of 30 mL. The fractions H56-58 (Hex:$CHCl_3$ 9:1) afforded **2** (45.0 mg) and the fractions H79-87 ($CHCl_3$) yielded 3,4-*seco*-friedelan-3-oic acid (**4**) (73.0 mg). The fractions H63-78 (Hex:$CHCl_3$ 1:1, 2.04 g) were re-submitted to a new silica gel CC (I) providing 186 fractions of 20 mL. Additional amounts of **2** (12.0 mg) and **3** (85.8 mg) were isolated from the fractions I53-55 (Hex:$CHCl_3$ 65:35) and I57-74 (Hex:$CHCl_3$ 65:35), respectively. The fractions G39-45 (Hex:$CHCl_3$ 8:2, 3.55 g) were re-chromatographed on flash silica CC (J, 100 fractions of 30 mL), providing 28-hydroxyfriedelan-3-one (**5**) (22.5 mg) from the fractions J46-67 (Hex:$CHCl_3$ 85:15). The fractions J68-84 (Hex:$CHCl_3$ 1:1, 113.3 mg) were re-submitted to a new flash silica gel CC (K), furnishing 77 fractions of 10 mL. The mixture of long chain fatty acid (**13**) (45.3 mg) was isolated from the fractions K53-55 ($CHCl_3$:EtOAc 8:2). The fractions G46-66 ($CHCl_3$ 7:3, 0.73 g) were re-submitted to a new flash silica CC (L) providing 37 fractions of 25 mL. The fractions L13-18 (Hex:$CHCl_3$ 8:2) yielded an additional amount of **5** (263.0 mg).

Part of the yellowish solid from the hexane branch extract (YBS, 1.8 g) after gutta removal was chromatographed on silica gel CC (M) resulting in 212 fractions of 30 mL. The fractions M123-125 ($CHCl_3$:EtOAc 9:1, 0.40 g) were re-chromatographed on flash silica CC (N) leading to 33 fractions of 10 mL. The fractions N19-29 ($CHCl_3$:EtOAc 7:3) were identified as **7** (283.2 mg). The fraction M129-130 ($CHCl_3$:EtOAc 8:2) yielded 21β-hydroxyfriedelan-3-one (**10**) (77.0 mg). The fractions M131-137 ($CHCl_3$:EtOAc 8:2, 0.14 g) were re-submitted to a new flash silica CC (O) leading to 59 fractions of 10 mL, furnishing a mixture (66.6 mg) of **8** and **9** from the fractions O34-41 ($CHCl_3$:EtOAc 8:2).

Part of the slightly greenish solid from hexane branch extract free of gutta (HBE, 14.2 g) was submitted to silica gel CC (P) furnishing 65 fractions of 250 mL. The fractions P31-32 (Hex:$CHCl_3$ 1:1, 5.33 g) were re-chromatographed on silica gel CC (Q) providing 90 fractions of 30 mL. The fractions Q52-59 (Hex:EtOAc 4:6, 1.20 g) were re-submitted to a new silica gel CC (R, 157 fractions of 10 mL) and only the fractions R119-129 ($CHCl_3$:EtOAc 6:4) yielded a pure compound, identified as **7** (598.8 mg). The fractions Q60-84 (Hex:EtOAc 1:9, 1.08 g) were re-subjected to a new silica gel CC (S, 75 fractions of 10 mL) providing a mixture of **2** and **3** (325.3 mg) from the fractions S46-47 ($CHCl_3$:EtOAc 7:3). The fractions S48-52 ($CHCl_3$:EtOAc 6:4, 450.0 mg) were re-submitted to a new silica gel CC (T, 78 fractions of 10 mL) providing a mixture of **8** and **9** (260.5 mg) (fractions T26-30, $CHCl_3$:EtOAc 95:5) and the pure compound **8** (85.3 mg) (fractions T38-46, $CHCl_3$:EtOAc 92:8). The fractions P33-39 (Hex:$CHCl_3$ 8:2, 2.35 g) were re-chromatographed on a new silica gel CC (U, 184 fractions of 15 mL). The fractions U105-114 ($CHCl_3$:EtOAc 4:6, 0.61 g) were submitted to another silica gel CC (V, 96 fractions of 10 mL) yielding additional amounts of **8** and **9** in a mixture (422.5 mg) from the fractions V29-35 ($CHCl_3$:EtOAc 9:1).

Cytotoxicity assay

Prior to the antiviral assays, the 50% cytotoxic concentration (CC_{50}) of the crude extracts of *T. micrantha* was established for the Vero cell lineage (ATCC CCL-81™). Vero cells were distributed into 96-wells microplates (4×10^5 cells *per* 100 µL *per* well) and incubated at 37 °C for 24 h. Then, 200 µL well^{-1} of DMEM (Dulbecco's minimum essential medium) with 5% FBS (fetal bovine serum, v v^{-1}) and the stock solution of the extracts dissolved in DMSO 20% in water (final DMSO concentration *per* well of 0.2%) were added starting with 1000 µg mL^{-1} in successive serial dilutions to 7.8 µg mL^{-1}. The employed solvent was used as a control (DMSO 0.2%), and the assays were performed in triplicate. After the 48 h incubation period, 25 µL of 3-(4,5-dimethyl-2-thiazolyl)-2,5-diphenyl-2*H*-tetrazolium bromide (MTT) solution (2 mg mL^{-1} in PBS) was added, and the plates were incubated at 37 °C for 90 min. Then, 130 µL of the solvent (DMSO) was added to

each well to dissolve the MTT-formazan crystals, and the cultures were kept under stirring at 150 rpm for 15 min. The CC_{50} was calculated using the absorbance ($\lambda = 492$ nm) in the wells, determined on a plate reader, as B/A × 100 (A = untreated cells; B = treated cells). The data presented are the means obtained from at least three experiments with internal triplicates.

Antiviral evaluation

Only *T. micrantha* extracts that presented a CC_{50} higher than 100 μg mL^{-1} were subjected to *in vitro* antiviral assays. Vero cells were distributed in a 96-wells microplate (4×10^5 cells *per* 100 μL *per* well) and incubated at 37 °C for 24 h. Then, the culture medium was removed, and 100 μL serial extract dilutions (250 to 15.6 μg mL^{-1}) were added to the wells. In a second 96-wells microplate, the same serial extract dilutions were mixed with the virus inoculums with a multiplicity of infection (moi), which corresponds to the average number of virus particles infecting each cell, of 0.1 virus $cell^{-1}$. Both 96-wells microplates were incubated at 5% CO_2 atmosphere at 37 °C for 30 min. Then, the suspension of the second microplate was transferred to the first microplate containing cells and incubated for 48 h at 37 °C. This procedure was done to ensure an adequate evaluation of the antiviral effect, investigating the extracts action in the virus and the cells to be infected throughout the multiplicative cycle of the virus. After 48 h of infection, the methodology for the cytotoxicity assay was used again to establish the median antiviral effective concentration (EC_{50}), which is the concentration that induced 50% protection of treated cells from viral infection. The EC_{50} was calculated using the absorbance ($\lambda = 492$ nm) in the wells, determined on a plate reader, as $[(A - B)/(C - B)] \times 100$ (A = treated and infected cells; B = untreated and infected cells; C = untreated and non-infected cells). The data presented are the means obtained from three experiments with internal triplicates.

Evaluation of the different stages in the viral infection cycle

In order to establish the antiviral effect, the cells and virus were incubated with active extracts at different stages of the viral infection cycle. At the adsorption stage, the cells were pretreated with the extracts before viral infection. At the penetration stage, the cells were infected with the virus before the addition of the extracts. The virucidal effect was also evaluated to verify if the extracts were capable of interacting with the virus at a stage prior to the viral infection of host cells. Then, the virus was incubated with the extracts before infecting the cells. The data presented are the means obtained from three experiments with internal triplicates.

Antiviral activity at the adsorption stage

The extracts in concentration ranging from 250.0 to 15.6 μg mL^{-1} (serial dilutions) were added to a monolayer cell (24-wells microplate, 5×10^5 cells $well^{-1}$) and maintained at 37 °C for 1 h in 5% CO_2 atmosphere. Then, the cells were washed and infected with ZIKV (moi = 0.1 virus $cell^{-1}$). After one hour of viral adsorption, the non-adsorbed viral inoculum was removed and the cells were washed with PBS before addition of 1 mL of semi-solid medium 199 containing 2% FBS, 2% CMC (carboxymethylcellulose, m v^{-1}). After 48 h, the cells were fixed with PBS/10% formaldehyde (v v^{-1}) for 30 min, washed and stained with 5% crystal violet solution (m v^{-1}) for 15 min. The viral lysis plaques were observed and compared with untreated and non-infected cells (cell control), cells treated with DMSO 0.2% and infected (vehicle control), cells treated with ribavirin 200 μg mL^{-1} and infected (drug control) and only infected cells (ZIKV control). Ribavirin (Sigma-Aldrich) was used as a negative control since it can inhibit the viral multiplication in the intracellular phase, but does not prevent viral adsorption.

Antiviral activity at the penetration stage

Vero cells were distributed in 24-wells microplates (5×10^5 cells *per* 100 μL *per* well) 24 h before the assay, then the cells were infected with ZIKV (moi = 0.1 virus $cell^{-1}$) without pretreatment and incubated at 4 °C for one hour. Then, the viral inoculum was removed and the cells were washed with PBS. The extracts in concentration ranging from 250.0 to 15.6 μg mL^{-1} (serial dilutions) were added to the infected cells and maintained at 37 °C for one hour in 5% CO_2 atmosphere. The extracts were removed, and the cells were washed with citrate buffer (pH 3) for 1 min. After, a semi-solid medium 199 containing 2% FBS, 2% CMC (m v^{-1}) and the antibiotic mixture were added to the plate, which was incubated at 37 °C for 48 h in 5% CO_2 atmosphere. The revelation methodology and control groups were the same as described for the adsorption assays.

Virucidal effect

The extracts were added to the viral inoculum at 37 °C for 1 h before cell infection. Then, they were placed in a 24-wells microplate containing Vero cells and incubated at 37 °C for 1 h in 5% CO_2. In the sequence, the viral inoculum

was removed, a semi-solid medium 199 containing 2% FBS and 2% CMC (m v^{-1}) was added and the microplate was maintained at 37 °C for 48 h in 5% CO_2 atmosphere. For the visualization of viral plaques, the cells were treated 48 h later by fixation with PBS/10% formaldehyde (v v^{-1}) and stained with 1% crystal violet solution (m v^{-1}) for 15 min. The control groups were the same as described for the adsorption assays.

Results and Discussion

Chemistry

The phytochemical study of hexane leaf and branch extracts of *T. micrantha* yielded ten friedelane triterpenes (**1** to **10**), the natural polymer gutta-percha (**11**), squalene (**12**), and a mixture of long-chain fatty acids (**13**) (Figure 1). All compounds are herein described for the first time as constituents of *T. micrantha*, as well as of the genus *Tontelea*. The chemical structures of these compounds were characterized by IR, GC, ^{1}H and ^{13}C NMR and through comparison with literature data.

The triterpene **1** was isolated as a white amorphous solid material with $[\alpha]_D^{21}$ +86.0 ($CHCl_3$) and mp 224-226 °C. Its molecular formula, $C_{30}H_{46}0_3$, was established by HR-ESI-MS (*m/z*: 477.3221 $[M + Na]^+$, calcd. 477.3339). The IR spectrum showed a large band at 1716 cm^{-1}, which was attributed to carbonyl groups. In this spectrum, the bands at 3548 and 3412 cm^{-1} were attributed to hydroxyl groups, probably due to the keto-enolic equilibrium. The ^{1}H NMR spectrum showed signals at δ_H 0.71, 1.05, 1.07, 1.09, 1.14, 1.16, 1.18 and 1.22, associated to eight methyl groups. Signals at δ_H 2.39 (1H, s), 2.58-2.61 (2H, m), 3.24 (1H, d, *J* 16.0 Hz) and 3.44 (1H, d, *J* 16.0 Hz) were correlated as α-carbonyl protons according to heteronuclear multiple bond correlation (HMBC) and heteronuclear single quantum correlation (HSQC) analyses. The ^{13}C NMR spectrum presented 30 signals that, with the aid of the distortionless enhancement by polarization transfer (DEPT)-135, were classified as 8 primary, 9 secondary, 4 tertiary and 9 quaternary carbon atoms, suggesting a friedelane skeleton.[20] Among the quaternary carbon atoms, three were characterized as carbonyl groups due to the chemical shifts at δ_C 202.73, 203.96 and 218.75. The hydroxyl groups suggested by the IR spectrum were absent in the NMR spectrum since no signals were observed for carbinolic carbon atoms. Probably, the hydroxyl bands were related to a keto-enolic equilibrium indicating triterpene **1** as a beta di-ketonic compound. In the HSQC spectrum, the signal at δ_C 7.29 (C-23) coupled with the doublet at δ_H 1.05 (H-23), which is a characteristic of the friedelane carbonyl C-3. In the HMBC spectrum, the signal of H-23 correlated with the signal at δ_C 203.96 (C-3), which coupled with signals at δ_H 2.58 (H-4), 3.24 (H-2) and 3.44 (H-2). Both H-2 correlated with a second carbonyl group at δ_C 202.73 (C-1), which coupled with the signal at δ_H 2.39 (H-10). These data confirmed the positions of the carbonyl groups at C-1 (δ_C 202.73) and C-3 (δ_C 203.96), confirming a beta di-ketonic compound. The third carbonyl group was attributed to C-21 due to the correlations between δ_H 1.07 (H-29), 1.18 (H-30), 1.60 (H-19β), 1.79 (H-22β), 1.83 (H-19α) and 2.60 (H-22α) with δ_C 218.78. In the nuclear Overhauser effect spectrum (NOESY), the signal at δ_H 3.44 (H-2) was attributed to H-2α due to the coupling with the signals at δ_H 2.58 (H-4) and 2.39 (H-10), so the signal at δ_H 3.24 was consequently attributed to H-2β. The coupling of δ_H 1.05 (H-23) with 2.58 (H-4), 0.71 (H-24) with 1.22 (H-25), 1.22 (H-25)/1.79 (H-18) with 1.09 (H-26), and 1.79 (H-18) with 1.16 (H-28) established a chair conformation to the rings B, C and D. The same conformation was assigned to ring E because of the couplings of δ_H 1.14 (H-27)/1.07 (H-29) with 2.60 (H-22α), and 1.14 (H-27) with 1.07 (H-29). The most important HMBC and NOESY correlations are shown in Figure 2.

After detailed analyses of 2D experiments, compound **1** was identified as friedelan-1,3,21-trione and its complete NMR spectral data are shown in Table 1.

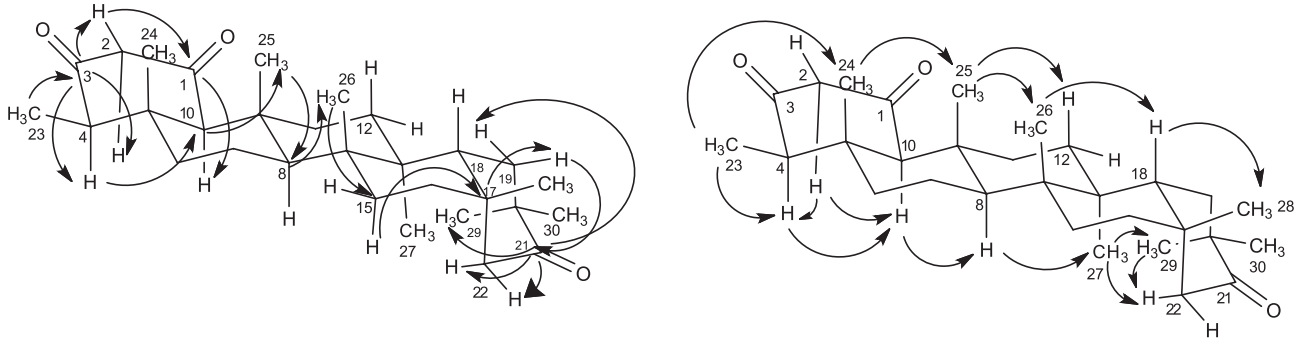

Figure 2. HMBC and NOESY correlations observed for friedelan-1,3,21-trione (**1**).

Table 1. NMR spectral data of friedelan-1,3,21-trione (**1**) and ^{13}C NMR data of 30-hydroxyfriedelan-3-one (**8**) (400 MHz, $CDCl_3$, δ is given in ppm)

Position	1						8	
	δ_C	Type	δ_H	HMBC (C→H)	COSY	NOESY	Type	δ_C
1	202.73	C	–	2, 10	–	–	CH_2	22.29
2	60.57	CH_2	3.24β (eq)	–	2	2α	CH_2	41.52
			3.44α (ax)		–	2β, 4, 10		
3	203.96	C	–	2, 4, 23	–	–	C	213.21
4	59.04	CH	2.58α (ax)	2, 10, 23, 24	23	2α, 6α, 10, 23	CH	58.24
5	37.83	C	–	4, 10, 24	–	–	C	42.15
6	40.52	CH_2	1.38α (ax)	24	6β	4, 6β	CH_2	41.30
			1.89β (eq)	–	6α , 7β	6α, 23, 24		
7	18.09	CH_2	1.29α (eq)	–	–	–	CH_2	18.25
			1.48β (ax)	–	6β, 8β	11β		
8	52.40	CH	1.26α (ax)	25, 26	7β	10, 27	CH	53.00
9	37.23	C	–	25	–	–	C	37.45
10	71.80	CH	2.39α (ax)	2, 4, 6, 24, 25	–	2α, 4, 8, 11α	CH	59.51
11	34.48	CH_2	1.18α (ax)	10, 25	11β, 12α	10, 11β	CH_2	35.58
			2.19β (eq)	–	11α , 12α , 12β	7β, 11α, 12β		
12	30.27	CH_2	1.29α (eq)	27	11β, 11α	–	CH_2	30.53
			1.49β (ax)	–	11β	11β, 25, 26		
13	39.72	C	–	26, 27	–	–	C	39.81
14	38.10	C	–	27	–	–	C	38.38
15	32.75	CH_2	1.33α (ax)	26	15β	15β, 27	CH_2	32.12
			1.55β (eq)	–	15α, 16β	15α, 26		
16	34.97	CH_2	1.38β (ax)	18, 28	15β, 16α	18, 28	CH_2	35.93
			1.76α (eq)	–	16β	–		
17	33.17	C	–	15, 16, 18, 19, 22, 28	–	–	C	30.00
18	41.82	CH	1.79β (ax)	16, 19, 22, 28	19	19β, 26, 28	CH	42.74
19	36.96	CH_2	1.60β (ax)	18, 29	18	18, 28	CH_2	29.34
			1.83α (eq)	–	–			
20	42.75	C	–	29, 30	–	–	C	33.38
21	218.78	C	–	19, 22, 29, 30	–	–	CH_2	28.17
22	54.97	CH_2	1.79β (eq)	28	22α	22α	CH_2	38.11
			2.60α (ax)	–	22β	22β, 27, 29		
23	7.29	CH_3	1.05	4	4	4, 6β, 24	CH_3	6.83
24	15.96	CH_3	0.71	4, 10	–	6β, 23, 25	CH_3	14.67
25	17.79	CH_3	1.22	10	–	12β, 24,26	CH_3	18.02
26	21.27	CH_3	1.09	15	–	12β, 15β, 18, 25	CH_3	19.97
27	18.55	CH_3	1.14	18	–	8, 15α, 22α, 29	CH_3	18.59
28	33.47	CH_3	1.16	22	–	16β, 18, 19β	CH_3	32.14
29	28.78	CH_3	1.07	30	–	22α, 27	CH_3	28.93
30	24.97	CH_3	1.18	29	–	–	CH_2	71.98

HMBC: heteronuclear multiple bond correlation; COSY: correlation spectroscopy; NOESY: nuclear Overhauser effect spectroscopy.

The known friedelane triterpenes **2** to **10** were isolated as white amorphous solid materials, pure or as mixtures. The structures of these compounds were determined comparing their respective NMR data with those previously published. Compounds **2**-**3** and **5**-**10** showed the duplet of methyl H-23, at the range of δ_H 0.8-0.9, confirming the presence of 5 rings in the friedelane skeleton. Compound **2** was identified as friedelan-3-one and **3** as 3β-friedelinol, mainly due to the carbonyl group at δ_C 213.20 and the hydroxyl group at δ_C 72.38, respectively.[20,21] The ^1H NMR spectrum of **5** presented seven signals of methyl groups and a singlet at δ_H 3.63 (2H), relative to a hydroxylated methylene carbon. Its ^{13}C NMR spectrum showed signals at δ_C 212.99 (C=O) and 68.08, which were attributed to

C-3 and C-28, respectively, characterizing the compound as 28-hydroxyfriedelan-3-one.[20] Compound **6** was identified as friedelan-3-oxo-28-al due to the aldehyde signal at δ_C 208.97 (HC=O) attributed to C-28.[22] Compound **7** showed two carbonyl groups at δ_C 212.85 and 218.74 in the ^{13}C NMR spectrum and was identified as friedelan-3,21-dione.[23] The ^{13}C NMR spectrum of **8** (Table 1) showed signals at δ_C 213.21 (C=O)/71.98 (CH_2OH) that were similar as the signals of 30-hydroxyfriedelan-3-one published by Magalhães *et al*.[24] However, the shifts of C12, C16, C19, C22, C26 and C27 were uncorrectly attributed in the literature, and after a detailed analysis of the 2D NMR the assignments were corrected and are presented in Table S1 (Supplementary Information). Based mainly on the signals at δ_C 213.07 (C=O) and 74.32 (CHOH), compound **9** was identified as 21α-hydroxyfriedelan-3-one.[25] For compound **10**, the signals at δ_C 213.17 (C=O) and 75.82 (CHOH) were coherent with the structure of 21β-hydroxyfriedelan-3-one.[26]

Compound **4** was identified as 3,4-*seco*-friedelan-3-oic acid due to the triplets at δ_H 0.79 (t, *J* 8.43 Hz, H-23) and 2.38 (t, *J* 8.50 Hz, H-2) together with the signal at δ_C 179.05, which was attributed to a carboxyl group.[27] The ^1H NMR spectrum of compound **11** showed an olefinic proton at δ_H 5.12 (t, 1H, *J* 6.4 Hz) and methylene groups at δ_H 1.98 (2H, m)/2.06 (2H, m). Also, the ^{13}C NMR spectrum presented signals associated to unsaturated carbon atoms at δ_C 124.25 and 134.93, allowing the identification of this compound as gutta-percha.[28] The ^1H NMR spectrum of compound **12** showed signals between δ_H 5.10-5.15 (6H, m), associated to protons bonded to C=C, and between δ_H 1.60-1.68, attributed to eight methyl groups, according to integrations. Moreover, the ^{13}C NMR spectrum showed signals at δ_C 124.30, 124.43, 131.25 and 135.12, which were attributed to unsaturated carbon atoms, identifying compound **12** as squalene.[29]

The ^1H NMR spectrum of mixture **13** indicated a long-chain fatty acid due to the signals of α-carboxylic protons (δ_H 2.34, 2H, t, *J* 7.2 Hz), β-carboxylic protons (δ_H 1.63, 2H, qt, *J* 8.0 Hz) and terminal methyl protons (δ_H 0.88, 3H, t, *J* 6.4 Hz). This was confirmed by the ^{13}C NMR spectrum because of the signals at δ_C 179.77 (C=O) and 14.24 (CH_3).[30] GC analysis revealed that the mixture **13** was mainly composed by 66% palmitic acid, 12% stearic acid and 11% oleic acid.

Antiviral activity

The cytotoxicity to Vero cells and global antiviral activity against ZIKV of the extracts of *T. micrantha* were evaluated by the cytotoxic concentration (CC_{50}), effective concentration (EC_{50}) and selective index (SI) values presented in Table 2. CC_{50} values higher than 100 μg mL^{-1} indicate a non-toxic extract.[31] On the other hand, lower values of EC_{50} display an effective antiviral activity. Moreover, the selective index (SI) was calculated by the ratio of the concentration of the extract that reduced cell viability to 50% (CC_{50}) to the concentration needed to inhibit the cytopathic effect to 50% (EC_{50}).

All leaf and branch extracts were non-toxic to Vero cells, once their values of CC_{50} were higher than 100 μg mL^{-1}. The values of EC_{50} varied from 38.53 to 83.05 μg mL^{-1} indicating that the extracts presented antiviral activity. The methanolic leaf extract (MLE) together with the hexane and chloroform branch extracts (HBE and CBE) showed the highest SI displaying a promising viral inhibitory effect. All extracts with an SI higher than three were evaluated at different stages of infection (adsorption and penetration of viral particle) and also for their virucidal effect.

At the ZIKV adsorption stage, the Vero cells were pretreated with the crude extracts prior to the infection to verify interactions with cellular receptors. The ELE and MLE showed a more pronounced activity than the other extracts with a protective concentration of the cells higher than 50% at 31.2 μg mL^{-1} (Figure 3). These concentration values of the leaf extracts are similar to those reported by Tan *et al*.[32] for the anti-parasitic drug suramin, which induced a ZIKV adsorption blockade of 80% at a concentration of 50.0 μg mL^{-1}. The CBE also showed a significant antiviral activity at the concentration

Table 2. Cytotoxic concentration (CC_{50}) to Vero cells, effective concentration (EC_{50}) against ZIKV and selectivity index (SI) of the extracts of *T. micrantha*

Extract			CC_{50} / (μg mL^{-1})	EC_{50} / (μg mL^{-1})	Selectivity index (SI)
Leaves	hexane	HLE	157.19 ± 14.23	59.09 ± 12.46	2.66
	ethyl acetate	ELE	224.96 ± 23.78	74.19 ± 4.92	3.03
	methanolic	MLE	351.47 ± 22.44	83.05 ± 12.05	4.23
Branches	hexane	HBE	181.91 ± 12.45	38.66 ± 4.94	4.70
	chloroform	CBE	370.78 ± 43.48	38.53 ± 8.21	9.60
	ethyl acetate	EBE	191.86 ± 37.09	67.34 ± 10.60	2.85

of 125.0 μg mL^{-1}, displaying lysis plates in smaller amounts when compared to the non-treated viral control. The HBE showed no activity at this stage.

In order to evaluate the penetration stage, the Vero cells were infected with ZIKV and incubated at 4 °C for one hour. This step was necessary because lower temperatures deactivate the enzymes responsible for the viral penetration, causing only viral adsorption on the cells. Then, the extracts were added to the microplates in serial dilutions and the temperature was raised to 37 °C to reactivate the enzymes. Both leaf extracts (ELE and MLE) protected the cell, even at the lowest concentration of 15.6 μg mL^{-1} (Figure 4) when compared to the viral control Ribavarin, an antiviral nucleoside analogue. The CBE partially inhibited the penetration of the virus at the concentration of 62.5 μg mL^{-1}. The HBE promoted a partial protection of the cells only at the highest tested concentration (250 μg mL^{-1}).

The ability to inhibit the viral multiplication cycle prior to the cell infection (virucidal effect) was assessed by adding serial dilutions of the extracts to the viral suspension (moi = 0.1 virus $cell^{-1}$) before incubation with Vero cells. All tested extracts inhibited 100% of the viral infection even at the lowest tested concentration (15.6 μg mL^{-1}) since no virus plaques were observed in the microplates (Figure 5).

This assay demonstrated that all extracts act mainly on the viral particle. In general, an efficient antiviral agent should inhibit viral multiplication without interfering directly in the host cell, enabling a cellular infection recovery and metabolic maintenance. However, the antiviral activity was also detected for the extracts at the adsorption and penetration stage, implying the possibility of a cellular component on the mechanism as well. In fact, antiviral effects have been reported to some Celastraceae family species. Kanyara and Njagi[33] demonstrated that *Maytenus buchanani* and *M. senegalensis* extracts were able to block HIV-10 viral infection, and Kohn *et al.*[12] showed bovine herpesvirus inhibition by extracts of *M. ilicifolia*. Nonetheless, this is the first time that the antiviral potential was reported for the *Tontelea* genus. Further studies concerning the antiviral activity of the isolated compounds and the phytochemical investigation of more polar extracts

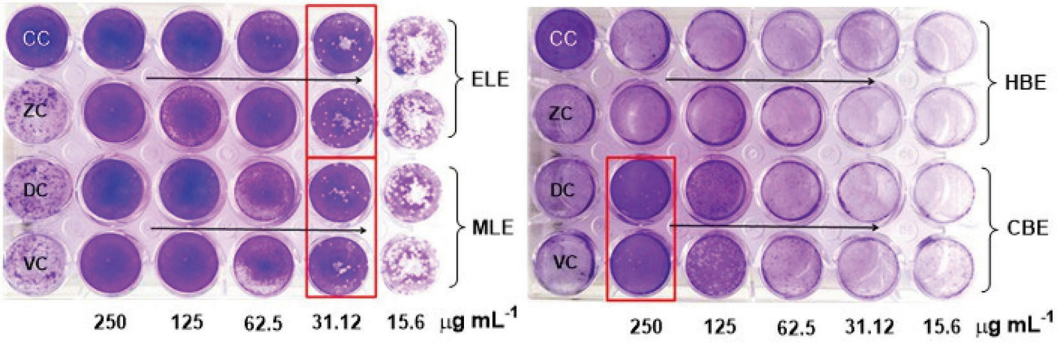

Figure 3. Effect of the extracts on cellular adsorption stage of the Zika virus. Decrease in cell damage by viral infection due to the increase in ELE, MLE, HBE and CBE extracts concentration. CC (cell control) = untreated and non-infected cells; VC (vehicle control) = infected cells treated with DMSO 0.2%; DC (drug control) = infected cells treated with ribavirin (200 μg mL^{-1}); ZC (Zika virus control) = cells infected by the virus, but non-treated. Ribavirin® was used as negative control due to its inhibition property of the viral multiplication in the intracellular phase. *Tontelea micrantha* samples: ELE = leaf ethyl acetate extract; MLE = leaf methanolic extract; HBE = branches hexane extract; CBE = branches chloroform extract.

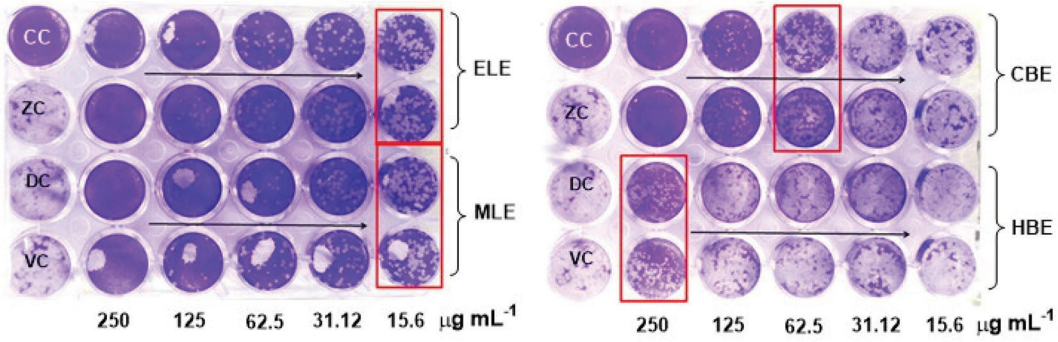

Figure 4. Effect of the extracts on the Zika virus cellular penetration stage. CC (cell control) = untreated and non-infected cells; VC (vehicle control) = infected cells treated with DMSO 0.2%, DC (drug control) = infected cells treated with ribavirin (200 μg mL^{-1}); ZC (Zika virus control) = cells infected by the virus, but non-treated. Ribavirin® was used as negative control due to its inhibition property of the viral multiplication in the intracellular phase. *Tontelea micrantha* samples: ELE = leaf ethyl acetate extract; MLE = leaf methanolic extract; HBE = branches hexane extract; CBE = branches chloroform extract.

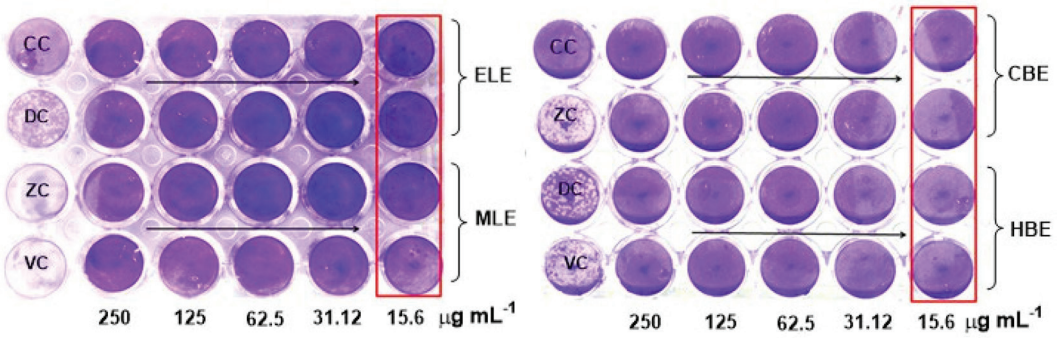

Figure 5. Virucidal effect of extracts on Zika virus particle. CC (cell control) = untreated and non-infected cells; VC (vehicle control) = infected cells treated with DMSO 0.2%; DC (drug control) = infected cells treated with ribavirin (200 μg mL^{-1}); ZC (Zika virus control) = cells infected by the virus, but non-treated. Ribavirin® was used as negative control due to its inhibition property of the viral multiplication in the intracellular phase. *Tontelea micrantha* samples: ELE = leaf ethyl acetate extract; MLE = leaf methanolic extract; HBE = branches hexane extract; CBE = branches chloroform extract.

are currently being performed in our laboratory, and the results will be reported in due course.

Conclusions

In this work, *Tontelea micrantha* was phytochemically studied for the first time. The new triterpene friedelan-1,3,21-trione (**1**), eleven known compounds and a mixture of long-chain fatty acids were isolated and chemically characterized. This is also the first report of these compounds for the *Tontelea* genus. Branch and leaf extracts were also tested for their activity against ZIKV in the early stages of viral infection and virucidal effect. They presented a virucidal effect, strongly acting on the viral particle, and inhibited the infection at the adsorption and penetration stages, except for the hexane branch extract. These results demonstrate that these extracts may be promising candidates for the ZIKV treatment.

Supplementary Information

Supplementary information is available free of charge at http://jbcs.sbq.org.br as a PDF file.

Acknowledgments

The authors thank to Fundação de Amparo à Pesquisa de Minas Gerais (FAPEMIG) for the financial support and Conselho Nacional de Desenvolvimento Científico e Tecnológico (CNPQ) for the scholarships (F. L. F.). The authors also thank Salomão B. V. Rodrigues for revising the English language and critical manuscript reviews.

References

1. Núñez, M. J.; Jiménez, I. A.; Mendonza, C. R.; Chavez-Sifontes, M.; Martinez, M. L.; Ichiishi, E.; Tokuda, R.; Tokuda, H.; Bazzocchi, I. L.; *Eur. J. Med. Chem.* **2016**, *111*, 95.
2. Veloso, C. C.; Soares, G. L.; Perez, A. C.; Rodrigues, V. G.; Silva, F. C.; *Rev. Bras. Farmacogn.* **2017**, *27*, 533.
3. Mercante-Simões, M. O.; Mazzottini, H. C. S.; Nery, L. A.; Ferreira, P. R. B.; Ribeiro, L. M.; Royo, V. A.; *An. Acad. Bras. Cienc.* **2014**, *86*, 1167.
4. Mercadante-Simões, M. O.; Paiva, E. A. S.; *Plant Species Biol.* **2015**, *31*, 117.
5. Araújo, A. R. B.; Royo, V. A.; Mercadante-Simões, M. O.; Fonseca, F. S. A.; Ferraz, V. P.; Oliveira, D. A.; Menezes, E. V.; Melo Júnior, A. F.; Brandão, M. M.; *S. Afr. J. Bot.* **2017**, *112*, 112.
6. Xiong, J.; Kashiwada, Y.; Chen, C. H.; Qian, K.; Natschke, S. L. M.; Lee, K. H.; Takaishi, Y.; *Bioorg. Med. Chem.* **2010**, *18*, 6451.
7. Qian, K.; Kuo, R. Y.; Chen, C. H.; Huang, L.; Morris-Natschke, S. L.; Lee, K. H.; *J. Med. Chem.* **2010**, *53*, 3133.
8. Silva, F. C.; Duarte, L. P.; Silva, G. D. F.; Filho, S. A. V.; Lula, I. S.; Takahashi, J. A.; Sallum, W. S. T.; *J. Braz. Chem. Soc.* **2011**, *22*, 943.
9. Niero, R.; Andrade, S. F.; Cechinel Filho, V.; *Curr. Pharm. Des.* **2011**, *17*, 1851.
10. González-Coloma, A.; López-Balboa, C.; Santana, O.; Reina, M. F.; *Phytochem. Rev.* **2011**, *10*, 245.
11. Veloso, C. C.; Rodrigues, V. G.; Azevedo, A. O. L.; Oliveira, C. C. O.; Gomides, L. F.; Duarte, L. P.; Duarte, I. D.; Klein, A.; Perez, A. C.; *J. Med. Plants Res.* **2014**, *8*, 68.
12. Kohn, L. K.; Queiroga, C. L.; Martini, M. C.; Barata, L. E.; Porto, P. S.; Souza, L.; Arns, C. W.; *Pharm. Biol.* **2012**, *50*, 1269.
13. Petersen, L. R.; Jamieson, D. J.; Powers, A. M.; Honein, M. A.; *N. Engl. J. Med.* **2016**, *374*, 1552.
14. Kindhauser, M. K.; Allen, T.; Frank, V.; Santhana, R. S.; Dye, C.; *Bull. W. H. O.* **2016**, *94*, 675.
15. Zanluca, C.; de Melo, V. C.; Mosimann, A. L.; dos Santos, G. I.; dos Santos, C. N.; Luz, K.; *Mem. Inst. Oswaldo Cruz* **2015**, *110*, 569.

16. Weaver, S. C.; Reisen, W. K.; *Antiviral Res.* **2010**, *85*, 328.
17. Yasuhara-Bell, J.; Yuanan, L.; *Antiviral Res.* **2010**, *86*, 231.
18. Figueiredo, J. N.; Räz, B.; Séquin, U.; *J. Nat. Prod.* **1998,** *61*, 718.
19. Rodrigues, V. G.; Duarte, L. P.; Silva, R. R.; Silva, G. D. F.; Mercadante-Simões, M. O.; Takahashi, J. A.; Matildes, B. L. G.; Fonseca, T. H. S.; Gomes, M. A.; Vieira Filho, S. A.; *Quim. Nova* **2015**, *38*, 237.
20. Mahato, S. B.; Kundu, A. P.; *Phytochemistry* **1994**, *37*, 1517.
21. Salazar, G. C. M.; Silva, G. D. F.; Duarte, L. P.; Vieira Filho, S. A.; Lula, I. S.; *Magn. Reson. Chem.* **2000**, *38*, 977.
22. Li, Y. Z.; Li, Z. L.; Yin, S. L.; Shi, G.; Liu, M. S.; Jing, Y. K.; Hua, H. M.; *Fitoterapia* **2010**, *81*, 586.
23. Patra, A.; Mukhopadhyay, A. K.; Mitra, A. K.; *Org. Magn. Reson.* **1981**, *17*, 166.
24. Magalhães, C. G.; Ferrari, F. C.; Guimarães, D. A. S.; Silva, G. D. F.; Duarte, L. P.; Figueiredo, R. C.; Filho, S. A. V.; *Rev. Bras. Farmacogn.* **2011**, *21*, 415.
25. Setzer, W. N.; Setzer, M. C.; Peppers, R. L.; McFerrin, M. B.; Meehan, E. J.; Chen, L.; Bates, R. B.; Nakkiew, P.; Jackes, B. R.; *Aust. J. Chem.* **2000**, *53*, 809.
26. Kaweetripob, W.; Mahidol, C.; Prawat, H.; Ruchirawat, S.; *Phytochemistry* **2013**, *96*, 404.
27. Vieira-Filho, S. A.; Duarte, L. P.; Santos, M. H.; Silva, G. D. F.; Lula, I. S.; *Magn. Reson. Chem.* **2001**, *39*, 746.
28. Ferreira, F. L.; Rodrigues, V. G.; Silva, F. C.; Matildes, B. L. G.; Takahashi, J. A.; Silva; G. D. F.; Duarte, L. P.; Oliveira, D. M.; Vieira-Filho, S. A.; *Rev. Bras. Farmacogn.* **2017**, *27*, 471.
29. Barreto, M. B.; Gomes, C. L.; Freitas, J. V. B.; Pinto, F. C. L.; Silveira, E. R.; Gramosa, N. V.; *Quim. Nova* **2013**, *36*, 675.
30. Couperus, P. A.; Clague, A. D. H.; Van Dongen, J. P. C. M.; *Org. Magn. Reson.* **1978**, *11*, 590.
31. Ramos, D. F.; Leitão, G. G.; Costa, F. N.; Abreu, L.; Villarreal, J. V.; Leitão, S. G.; Said y Fernández, S. L.; Silva, P. E. A.; *Rev. Bras. Cienc. Farm.* **2008**, *44*, 669.
32. Tan, C. W.; Sam, I. C.; Chong, W. L.; Lee, V. S.; Chan, Y. F.; *Antiviral Res.* **2017**, *143*, 186.
33. Kanyara, J. N.; Njagi, E. N. M.; *Phytother. Res.* **2005**, *19*, 287.

Submitted: July 4, 2018
Published online: October 18, 2018